



Novel ultrastructural findings on cardiac mitochondria of huddling Brandt's voles in mild cold environment

Zhe Wang¹, Jin-hui Xu^{*,1}, Jun-jie Mou¹, Xiao-tong Kong, Jian-wen Zou, Hui-liang Xue, Ming Wu, Lai-xiang Xu

College of Life Sciences, Qufu Normal University, 273165 Qufu, Shandong, China

ARTICLE INFO

Keywords:

Huddling
Apoptosis
Mitochondrial fission
Low temperature
Heart
Mitochondrial autophagy

ABSTRACT

Reduced ambient temperature has a damaging effect on mammalian myocardium. Huddling as a cooperative behavior has evolved in social mammals as a strategy to maximize adaptation to environmental cooling. Here, we studied the effects of huddling behavior on mitochondrial morphology, number, and function in the myocardia of Brandt's voles (*Lasiopodomys brandtii*) under cool environmental temperatures (15 °C). Results showed (1) mitochondrial swelling and cristae disruption in the cool huddling group (CH) and cool separated group (CS). Compared to the control group (CON, 22 °C), damaged mitochondria in the cool huddling and separated groups reached > 90%; however, total number of mitochondria in the CH group was similar to that in the CON group. (2) ATP synthase activity was lowest in the CS group, whereas citrate synthetase activity was maintained among the three treatment groups. (3) Bax/bcl2 protein expression in the CH and CS groups was higher than that in the CON group, whereas DNA fragmentation, nuclear number, and caspase3 activity showed no significant differences among the three groups. (4) The protein expression levels of dynamin-related protein1 and mitochondrial fission factor were highest in the CH group. (5) Both protein expression of PINK1 and phosphorylation ratio of Parkin showed the pattern CS > CH > CON. (6) Total number of mitochondria was higher in males than in females. In general, the increased mitochondrial fission level observed in huddling voles partially counteracted the decrease in myocardial mitochondria caused by the increase in autophagy.

1. Introduction

Reduced ambient temperature is a stress stimulus for mammals, especially small mammals, as energy requirements per unit of body mass are high due to the large surface area to volume ratio. Moreover, when environmental stressors persist for prolonged periods, small animals will be challenged and their tissues and organs are more vulnerable to the impact of external environmental temperature (Gilbert et al., 2010). Hypothermia can result in a slow heart rate, decreased blood flow output, and decreased myocardial contraction and relaxation (Chavez et al., 2017; Kelly and Nolan, 2010; Polderman, 2009; Tessier and Storey, 2012; Treat et al., 2018). Due to the high surface area to volume ratio, the cardiac muscle of small mammals is more susceptible to low external temperatures. After 16 days (d) of hypothermia treatment (−7 °C), the myocardial ultrastructure in rats showed instability of mitochondrial membranes, with some mitochondria undergoing complete or partial destruction (Lushnikov and Nepomniashchikh, 1991). Mild cooling (from 32 °C to 23 °C) for 27 d led to a reduction in

H₂O₂ in the cardiac muscle of Brandt's voles (*Lasiopodomys brandtii*), thus indicating a decrease in mitochondrial oxidation ability (Xu et al., 2019). Thus, these studies suggest that the effects of hypothermia on cardiac muscle may involve changes in mitochondria.

Mitochondria are responsible for aerobic oxidation and mitochondrial damage can weaken the energy supply of muscle fibers (Dugbartey et al., 2017; Fang et al., 2011; Kenny et al., 2017). Citrate synthase is a limiting enzyme of the tricarboxylic acid cycle (Remington, 1992; Wiegand and Remington, 1986) and ATP synthase is a rate-limiting enzyme in the ATP synthesis pathway (Kramarova et al., 2008). Thus, studies on citrate synthase and ATP synthase can partly measure changes in mitochondrial oxidative metabolism and energy supply of the cardiac muscle under a cool environment.

The destruction of mitochondria may play a role in the balance of apoptosis, mitochondrial autophagy, and fission. Bax is one of the most important apoptotic molecules in mammals. It is inserted into the outer membrane of mitochondria via bax/bax-homo-oligomerization, eventually leading to mitochondrial swelling, and can also indirectly

* Corresponding author.

E-mail address: xujinhui@qfnu.edu.cn (J.-h. Xu).

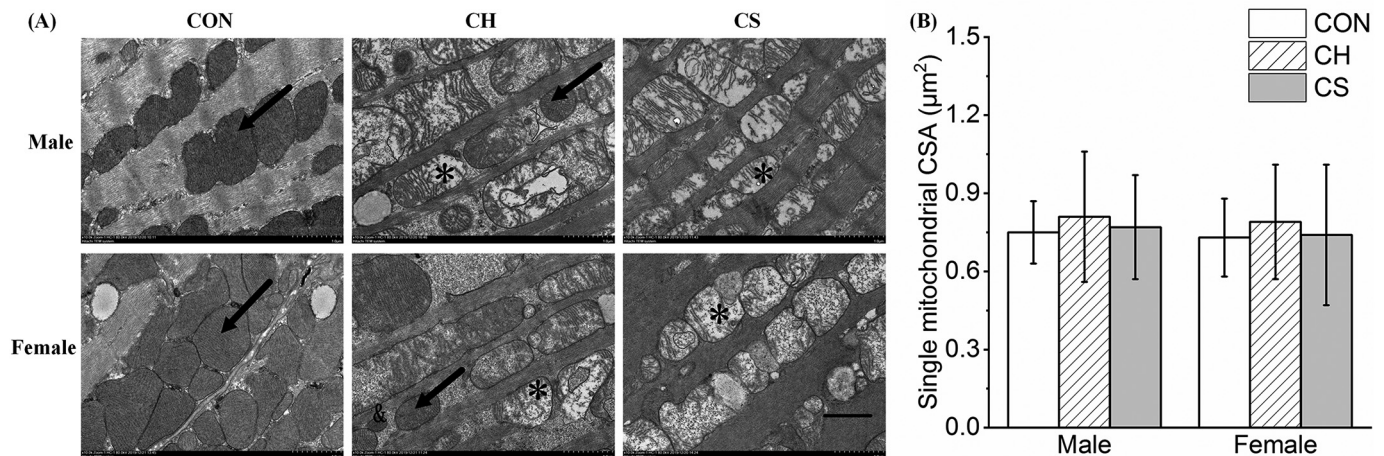
¹ Zhe Wang, Jin-hui Xu and Jun-jie Mou contributed equally to this work.

Table 1

Effects of cool environment on body weight (BW), myocardium weight (MW), and MW to BW ratio (MW/BW) in voles after eight weeks.

Group	Male			Female			Significance between sexes
	CON	CH	CS	CON	CH	CS	
BW before treatment (g)	39.56 ± 8.23	37.35 ± 7.82	37.67 ± 8.56	33.51 ± 10.87	34.2 ± 6.27	32.79 ± 4.68	*
BW after treatment (g)	38.44 ± 7.93	31 ± 4.85	33.47 ± 5.88	32.20 ± 10.91	28.5 ± 5.89	28.63 ± 4.62	*
myocardium weight (g)	0.18 ± 0.02	0.17 ± 0.02	0.16 ± 0.02	0.16 ± 0.03	0.17 ± 0.03	0.16 ± 0.02	ns
MW/BW (mg/g)	4.6 ± 0.29	5.3 ± 0.67	4.9 ± 0.33	5.1 ± 0.44	5.8 ± 0.88	5.5 ± 0.27	*

CON, control group; CH, cool huddling group; CS, cool separated group. *, $P < .05$ significant difference between males and females; ns, no significant difference between males and females.

**Fig. 1.** Changes in single mitochondrion cross-sectional area in voles.

(A) Cristae of myocardial mitochondria ultrastructure. Scale bar = 1 μm . Arrow shows normal mitochondria with clear cristae and intact membranes. In CH and CS groups, mitochondria (*) were swollen and cristae were disordered. Small mitochondria (&) with complete morphology and structure can be seen in CH. (B) Bar graph of single mitochondrion cross-sectional area in voles. Values are means \pm SD. Six figures were analyzed in each sample; eight samples were analyzed in each group. CON, control group; CH, cool huddling group; CS, cool separated group.

activate caspase3, resulting in nuclear DNA fragmentation, i.e., apoptosis (Fu et al., 2016; Wang et al., 2020). Furthermore, bcl2 inhibits apoptosis via suppression of bax/bax-homo-oligomerization (Antonsson et al., 1997; Korsmeyer et al., 1993). Excessive accumulation of the PTEN induced putative kinase 1 (PINK1) protein can directly and indirectly phosphorylate Parkinson's disease protein 2 (Parkin) and promote the formation of mitochondrial autophagy (Kane et al., 2014; Yamano et al., 2016). Dynamin-related protein 1 (DRP1) is the GTP-hydrolyzing mechanoenzyme that catalyzes mitochondrial fission in the cell that drives division via GTP-dependent constriction (Kraus and Ryan, 2017; Michalska et al., 2016; Otera et al., 2013; Tilokani et al., 2018). The DRP1 receptor mitochondrial fission factor (MFF) is a major regulator of mitochondrial fission, and its overexpression results in increased fission (Fekkes et al., 2000; Mozdy et al., 2000; Tieu and Nunnari, 2000). In contrast, the DRP1 receptor fission 1 (FIS1) appears to recruit inactive forms of DRP1 and its overexpression inhibits mitochondrial fission (Liu and Chan, 2015). Thus, studies of these factors are helpful to explore apoptosis, mitochondrial autophagy, and fission levels.

Huddling is a social thermoregulatory behavior, which can be defined as an "active and close aggregation of animals". It is a cooperative group behavior, permitting individuals involved in social thermoregulation to minimize heat loss and thereby lower their energy expenditure, and possibly allowing them to reallocate saved energy to other functions (Douglas et al., 2017; Gilbert et al., 2010). It is commonly used by small mammals and birds to reduce heat loss and energy expenditure in the cold (Jefimow et al., 2011; Sukhchuluun et al., 2018; Wojciechowski et al., 2011; Zhang et al., 2018). Research has shown that many mammals, such as Brandt's voles (*Lasiopodomys brandtii*), degu (*Octodon degus*), Damaraland mole-rat (*Cryptomys damarensis*),

and Natal mole-rat (*Cryptomys hottentotus natalensis*), huddle when the ambient temperature is lower than 15–20 $^{\circ}\text{C}$, and their energy-saving can reach 30% (Kotze et al., 2008; Nunez-Villegas et al., 2014; Sukhchuluun et al., 2018). Research on Eastern pygmy possums (*Cercartetus nanus*) has shown that huddling at mild low temperatures (14 $^{\circ}\text{C}$) can reduce energy consumption by up to 50% (Namekata and Geiser, 2009). The benefits of huddling in energy conservation, local environmental heating, and survival have also been studied in several species (Kotze et al., 2008; Nowack and Geiser, 2016; Scantlebury et al., 2006). Overall, huddling individuals exhibit increased survival, lower food intake, decreased body mass loss, increased growth rate, and more constant body temperature, as well as a significant reduction in metabolic rate (Gilbert et al., 2010). Various studies have reported on the morphological and physiological changes in animal bodies; to date, however, no studies have reported on myocardial mitochondria in huddling mammals under different temperatures.

Brandt's voles are small non-hibernating herbivorous rodents, which are widely distributed in the Inner Mongolian grasslands of northern China, dry steppe zone of Mongolia, and southeast Baikal region of Russia. These highly socialized animals exhibit huddling behavior in winter as an adaptation to their harsh habitat environments (Zhang et al., 2018). Studies have shown that mild cooling can significantly change the level of oxidative stress in the cardiac muscle of Brandt's voles (Xu et al., 2019). Furthermore, their metabolic rate and thermogenic capacity decreased while activity increased in huddling groups compared with separate individuals at low temperatures, suggesting that huddling is a good strategy for small mammals to cope with cold environments (Sukhchuluun et al., 2018). However, the roles of the morphology and function of myocardial mitochondria in this adaptive strategy have not yet been reported. Therefore, we hypothesized that a

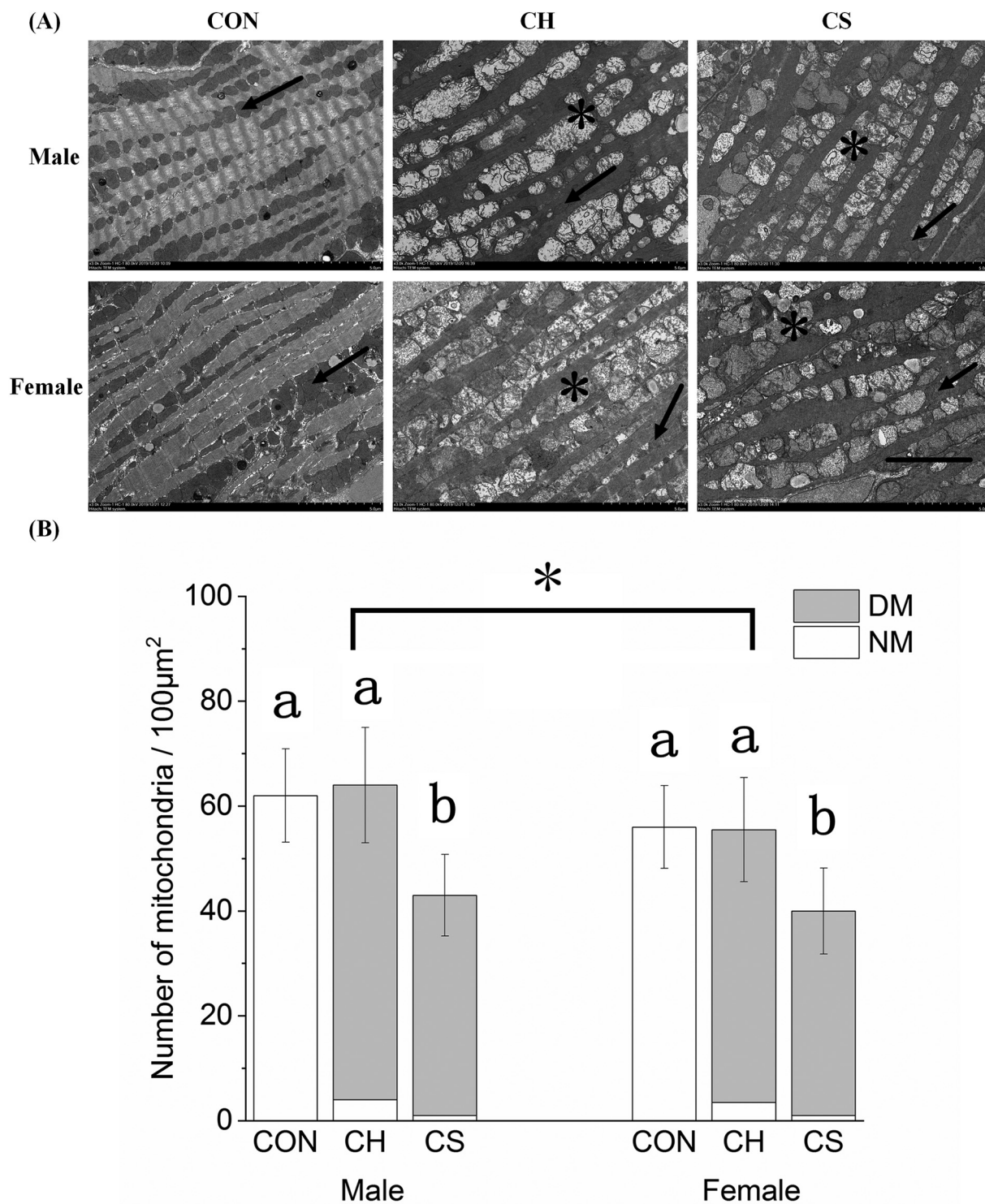


Fig. 2. Changes in number of myocardial mitochondria in voles.

(A) Myocardial mitochondria ultrastructure in voles from three temperature groups. Arrow shows normal mitochondria with clear cristae and intact membranes. In CH and CS groups, mitochondria (*) were swollen and cristae were disordered. Scale bar = 5 μm. (B) Bar graph of number of normal and damaged mitochondria. Values are means ± SD. Six figures were analyzed in each sample; eight samples were analyzed in each group. NM, normal mitochondria; DM, damaged mitochondria; CON, control group; CH, cool huddling group; CS, cool separated group. Different letters identify statistically significant differences among temperature treatment groups ($P < .05$). *, $P < .05$ significant difference between males and females.

cool environment will damage myocardial mitochondria in Brandt's voles. We also hypothesized that huddling will effectively alleviate this damage. To test these hypotheses, we observed the ultrastructure of the cardiac muscle in huddling and individual Brandt's voles under mild

temperature differences (normal 22 °C; cool 15 °C) in autumn. We also determined the protein expression levels or activity of apoptosis, mitochondrial function, autophagy, and fission-related signals. We further explored the molecular mechanism related to the effects of a mild cold

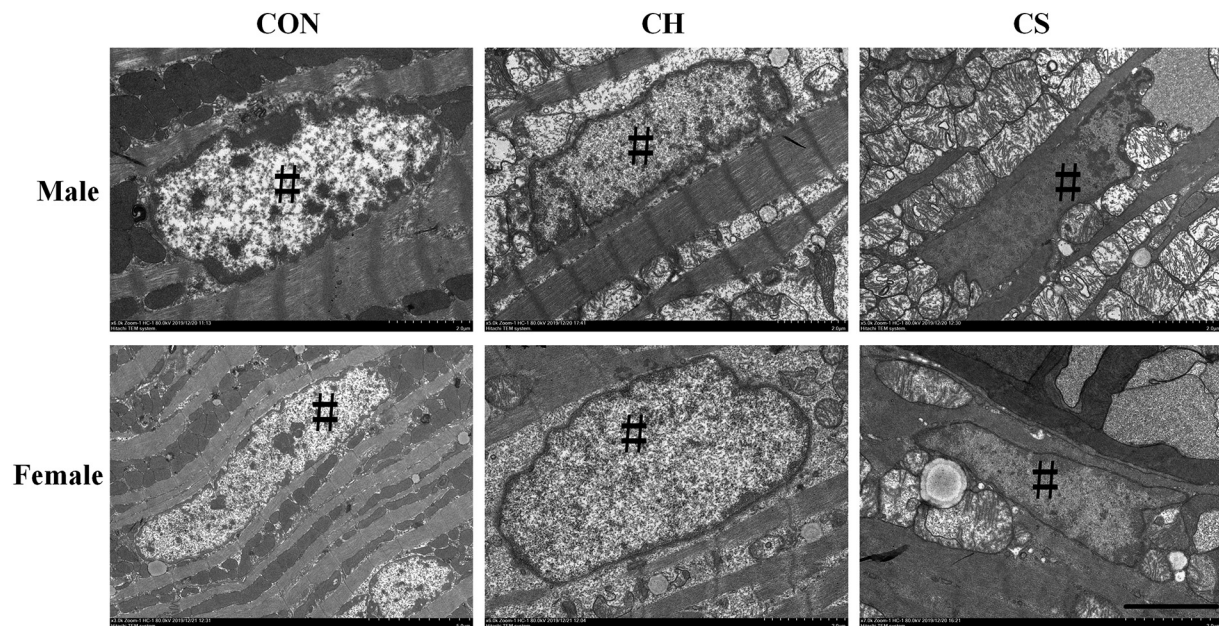


Fig. 3. Myocardial nucleus ultrastructure in voles.

Scale bar = 2 μ m. Myocardial nucleus (#) is distributed between myofilaments. CON, control group; CH, cool huddling group; CS, cool separated group.

environment and huddling habit on the structure and function of myocardial mitochondria.

2. Materials and methods

2.1. Ethics statement

All procedures followed the Laboratory Animal Guidelines for the Ethical Review of Animal Welfare (GB/T 35892–2018) and were approved by the Animal Care and Use Committee of Qufu Normal University (Permit Number: dwsc 2,019,012).

2.2. Animals and groups

In early September 2019, Brandt's voles were captured using live trapping from an enclosure at the Inner Mongolia Grassland Animal Ecology Research Station (60 \times 80 m), located in the Maodeng pasture (44°11'N, 116°27'E; 1100 m elevation) of Xilinhot, Inner Mongolia, China. The voles were acclimated under laboratory conditions for two weeks. They were housed with four animals per cage (28 \times 18 \times 12 cm) at an ambient temperature of 22 \pm 2 $^{\circ}$ C, relative humidity of 55% \pm 5%, and light regime of 12:12 hours light/dark (light on from 06:00 to 18:00). Food (standard rabbit chow, Pengyue Experimental Animal Breeding Co., Ltd., China) and water were provided ad libitum and wood shavings were used as bedding.

Based on body weight and degree of wear on upper molars, a total of 24 adult male voles (28–50 g, average 38 g) and 24 adult female voles (27–54 g, average 33 g) were randomly divided into three groups, respectively. Voles in the control group (CON) were continuously housed at an ambient temperature of 22 \pm 2 $^{\circ}$ C, with four animals per cage (two males and two females), as group activity of voles in this environment but not huddling, it was similar to its normal state in autumn. Two groups of each sex were transferred to the cool cabinet in different grouping conditions (huddling and separated). Voles from the cool separated group (CS) were housed individually in cages, whereas four (two males and two females) voles from the cool huddling group (CH) were housed together in a cage. Group size (four voles in each cage) ensured most animals remained inactive in a huddle (Sukhchuluun et al., 2018). The temperature in the cabinet was set to 15 $^{\circ}$ C. Animal treatment started in late September and lasted for eight

weeks.

2.3. Sample preparation

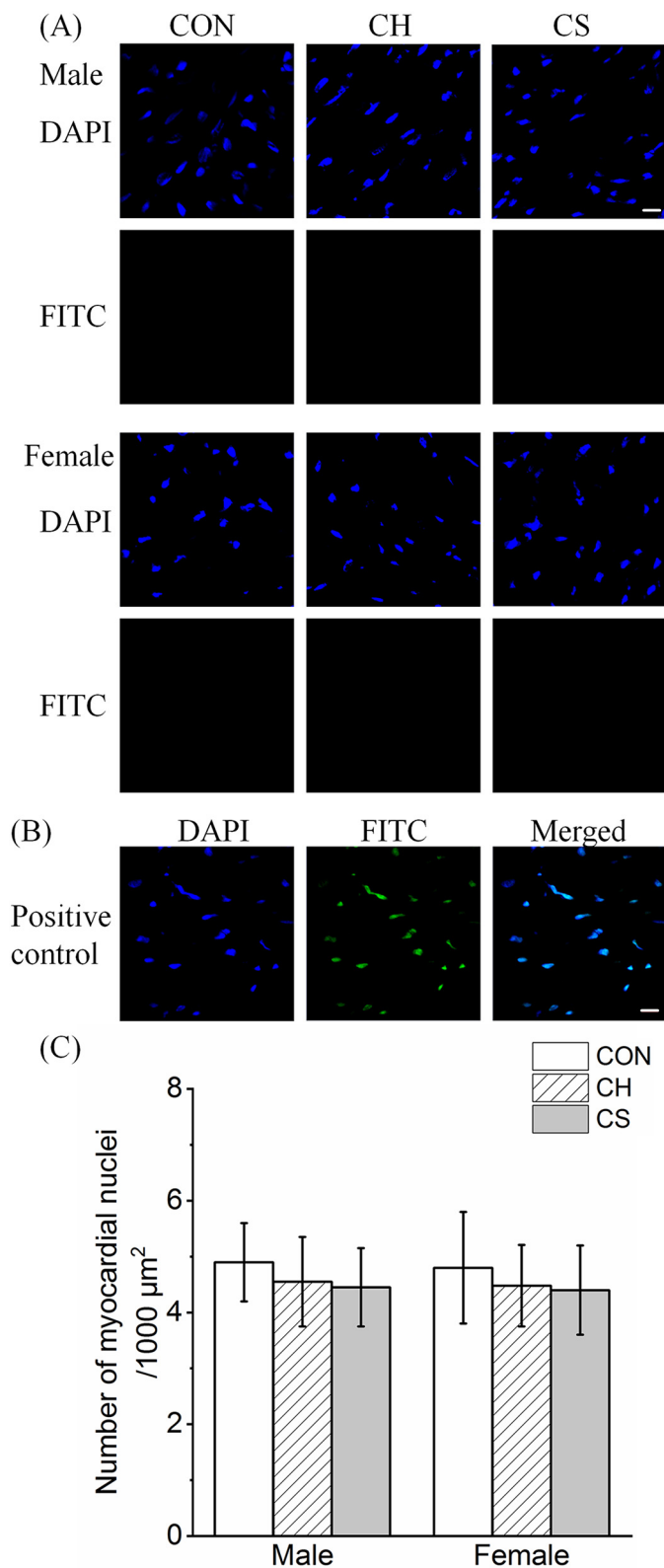
All animals were sacrificed by CO₂ asphyxiation between 08:00 and 11:00 on the last day (Sukhchuluun et al., 2018; Wang et al., 2020). After the rapid removal of the cardiac muscle, part of the ventricles was immediately cut off and fixed by glutaraldehyde. The rest of the cardiac muscle was frozen with liquid nitrogen and store at -80° C. Specimens were fixed in 1% osmium tetroxide in the same buffer, dehydrated with a graded series of ethanol, and embedded in epoxy resin. All procedures were carried out in accordance with the approved guidelines.

2.4. Transmission electron microscopy (TEM)

The cardiac muscle was cut to blocks and immersed in 3% glutaraldehyde-paraformaldehyde. The blocks were then dehydrated with a graded series of ethanol and embedded in epoxy resin, with TEM then performed as described previously (Wang et al., 2019). A semithin section was applied to tissue samples, and after methylene blue staining (Biazik et al., 2015), the sections were adjusted under the microscope and sliced with an ultramicrotome (LKB-NOVA, USA). The ultrathin sections were then double-stained with Reynolds' lead citrate and ethanolic uranyl acetate (Reynolds, 1963) and examined via TEM (Hitachi, HT7800, Japan). Images were processed with NIH Image-Pro Plus 6.0 and then analyzed using the measurement tools provided by this software. Mitochondrial subpopulation densities were determined within a defined region (100 μ m² area) at a minimum of three locations within an image taken at 7000 \times magnification. For the mitochondrial cross-sectional area (CSA), six images were analyzed for each sample, and the CSA of all complete mitochondria (about 10) within each image was randomly selected and analyzed. Thus, the CSAs of \sim 60 mitochondria per sample were determined. Eight samples were analyzed in each group.

2.5. Terminal deoxynucleotidyl transferase biotin-dUTP nick end-labeling (TUNEL) staining and number of nuclei

DNA fragmentation induced by apoptosis was determined by double-labeled fluorometric TUNEL detection, and evaluation was done



as described previously (Wang et al., 2020). Briefly, 10- μ m thick frozen tissue cross-sections were air-dried and fixed in 4% paraformaldehyde in phosphate-buffered saline (PBS, pH 7.4) at room temperature for 20 minutes. The sections were then permeabilized with 0.2% Triton X-100 in 0.1% sodium citrate at 4 °C for 2 min. Subsequently, TUNEL

Fig. 4. Fluorescent terminal deoxynucleotidyl transferase biotin-dUTP nick end-labeling (TUNEL) staining in cardiac muscle of voles.

(A) TUNEL staining in cardiac muscle of voles. Scale bar = 20 μ m. Blue represents 4'6'-diamidino-2-phenylindole (DAPI)-stained nucleus, green represents TUNEL by FITC. (B) Positive control of TUNEL staining in cardiac muscle of voles. Scale bar = 20 μ m. Blue represents DAPI-stained nucleus, green represents TUNEL by FITC, and merged represents the co-localization of nucleus and TUNEL. (C) Bar graph of number of myocardial nuclei in voles. Values are means \pm SD. Six figures were analyzed in each sample; eight samples were analyzed in each group. CON, control group; CH, cool huddling group; CS, cool separated group.

(#MK1023, Boster, Wuhan, China) reaction mix was added at the recommended 1:9 ratio, and the sections were incubated for 60 min at 37 °C in a humidified chamber in the dark according to the manufacturer's protocols. Finally, the sections were counterstained with DAPI. Positive and negative controls were included in each experiment. Sections were treated with DNase I (Tiangen, Beijing, China) in DNase buffer for 10 min at room temperature before incubating with the TUNEL reaction mix (positive control) or without the TdT enzyme (negative control). Images were visualized using a confocal laser scanning microscope (Olympus, Osaka, Japan) at an objective magnification of 40 \times . The number of nuclei was determined within a defined region (2500 μ m² area) at a minimum of three locations within an image taken at 400 \times magnification. Six figures were analyzed in each sample, and eight samples were analyzed in each group.

2.6. ATP synthase, Citrate synthase, and caspase3 activity

Samples stored at -80 °C were used to detect ATP synthase, citrate synthase, and caspase3 activity. ATP synthase activity was determined by measuring free phosphate group at 450 nm using an ATP synthase Activity Assay Kit (H-172421, Shanghai Hengyuan Biological Technology Co., Ltd., China) according to the manufacturer's instructions (OuYang et al., 2018). Citrate synthase activity was determined by measuring coenzyme A formation at 450 nm with a Citrate Synthase Activity Assay Kit (H-109821, Shanghai Hengyuan Biological Technology Co., Ltd., China) according to the manufacturer's instructions (Song et al., 2018). Caspase3 activity in cell lysates was determined using a Caspase3 Activity Kit (BC3830, Solarbio, Beijing, China) following the manufacturer's protocols (Xu et al., 2018).

2.7. Western blotting

Total protein was extracted from the tissues and solubilized in sample buffer (100 mM Tris, pH 6.8, 5% 2- β -mercaptoethanol, 5% glycerol, 4% SDS, and bromophenol blue), with the extracts of cardiac protein then resolved via SDS-PAGE (10% Laemmli gel with an acrylamide/bisacrylamide ratio of 29:1 and 98% 2,2,2-trichloroethanol (Aladdin, J1522028, China)). Due to the study of protein expression in different tissues, we used total protein content as a reference. After electrophoresis, the gel was irradiated on the UV platform of the electrophoresis gel imaging analysis system (Bio-Rad, California, USA) for 5 min, after which the signal was collected. As described in the references (Li and Shen, 2013; Posch et al., 2013), the original image captured with no gain was stored. After that, the fluorescent intensity of each lane (removing fluorescent intensity of background) was determined using Image-Pro Plus 6.0, which has an internal reference to correct the fluorescence intensity of the target protein. The proteins were then electrically transferred to PVDF membranes (0.45- μ m pore size) using a Bio-Rad wet transfer apparatus. The blotted membranes were blocked with 5% skimmed milk powder in Tris-buffered saline (TBS; 150 mM NaCl, 50 mM Tris-HCl, pH 7.5) and incubated with rabbit anti-ATP synthase (1:1000, #14676, Proteintech, Wuhan, China), rabbit anti-citrate synthase (1:1000, #16131, Proteintech), rabbit anti-bax (1:1000, #50599, Proteintech), rabbit anti-bcl2

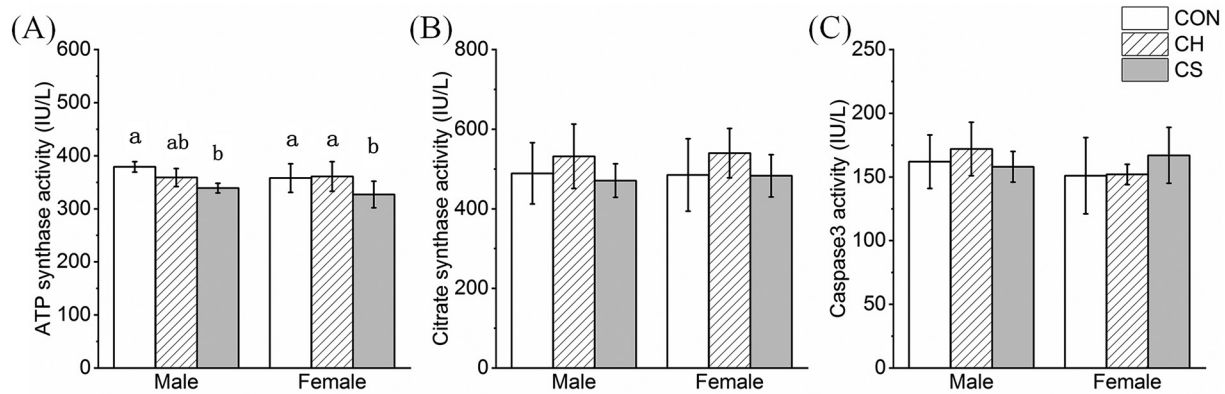


Fig. 5. ATP synthase (A), citrate synthase (B), and caspase3 (C) activity in cardiac muscle of voles. Values are means \pm SD. $n = 8$. CON, control group; CH, cool huddling group; CS, cool separated group. Different letters indicate significant differences among temperature treatment groups ($P < .05$).

(1:1000, #3498, Cell Signaling Technology CST, Danvers, MA, USA), rabbit anti-DRP1 (1:1000, #12957, Proteintech), rabbit anti-MFF (1:1000, #17090, Proteintech), rabbit anti-FIS1 (1:1000, #10956, Proteintech), rabbit anti-PINK1 (1:1000, #23274, Proteintech), rabbit anti-parkin (1:1000, #14060, Proteintech), and rabbit anti-phosphoparkin (1:1000, AF3500, Affinity Biosciences, OH, USA) in TBS containing 0.1% bovine serum albumin (BSA) at 4 °C overnight. The membranes were then incubated with IRDye 800 CW goat anti-rabbit secondary antibodies (1:5000, #31460, Thermo Fisher Scientific, Rockford, IL, USA) for 90 min at room temperature and visualized with an Odyssey scanner (Bio-Rad, California, USA). Quantification analysis of the blots was performed using NIH Image J software (Image-Pro Plus 6.0).

2.8. Statistical analyses

The normality of data and homogeneity of variance were determined using Shapiro-Wilk and Levene tests, respectively. All data exhibited normal distribution and variance was homogeneous. Double factor variance analysis (two-way ANOVA) was used to compare the differences in treatment and sex. Results were significant at $P < .05$. Data are expressed as means \pm standard deviation (Mean \pm SD). All statistical analyses were conducted using SPSS 19.0.

3. Results

3.1. Vole body weight (BW), myocardium weight (MW), and MW to BW ratio (MW/BW)

No significant differences in BW were observed among the three groups before the experiment. After two months of cool environment treatment, the BW, MW, and MW/BW values still showed no significant differences among the three treatment groups. However, the BW values were higher in males than in females and the MW/BW ratio was higher in females than in males (Table 1).

3.2. Ultrastructural changes in myocardial mitochondria

Mitochondrial morphology showed a similar trend between males and females. In the CON group, the mitochondrial membrane was intact and smooth, and the cristae were clear and filled with a mitochondrial inner membrane. In the CH and CS groups, mitochondrial swelling and cristae disruption were observed. In the CH group, mitochondria with smooth membranes and clear cristae were occasionally observed, whereas these normal mitochondria were rarely observed in the CS group. Small mitochondria with complete morphology and structure

were seen in the CH group. In addition, vacuolation of mitochondria was observed in the cardiac muscle of the CS group, indicating significant degenerative changes (Fig. 1A). Single mitochondrion CSA showed no significant differences among the three treatment groups in male and female voles (Fig. 1B).

Most of the myocardial mitochondria in voles were distributed between the muscle filaments (Fig. 2A). Total number of myocardial mitochondria showed a similar trend in male and female voles. Furthermore, total number was significantly lower in the CS group compared with the other groups but showed no significant differences between the CON and CH groups. In addition, the ratio of normal myocardial mitochondria in male and female voles in the CH group was similar (6.6% in males and 6.7% in females), but was significantly higher ($P < .05$) than that in the CS group (2.3% in males and 2.5% in females) for both males and females. Thus, there was a significant difference in the total number of mitochondria between males and females (Fig. 2B).

3.3. Ultrastructural changes in myocardial nuclei

Myocardial nuclei were mostly distributed between myofilaments, with almost no chromatin agglutination or nuclear damage observed in the three treatment groups (Fig. 3).

3.4. DNA fragmentation

TUNEL staining can provide direct evidence of apoptosis. In the three treatment groups of males and females, no significant DNA fragmentation was observed in random myocardial sections (Fig. 4A and B). In addition, there was no significant change in the number of nuclei among the three treatment groups (Fig. 4C).

3.5. Changes in ATP synthase, CS, and caspase3 activity

ATP synthase activity in the CON group was significantly higher than that in the CS group ($P < .05$) (Fig. 5A). However, CS and caspase3 activity showed no significant differences among the three groups for both males and females (Fig. 5B and C).

3.6. Changes in protein expression of mitochondrial function-related proteins

The relative protein expression levels of ATP synthase and citrate synthases were detected by western blot analysis, as shown in Fig. 6A. Representative polyacrylamide gels of total protein are shown in Fig. 6B.

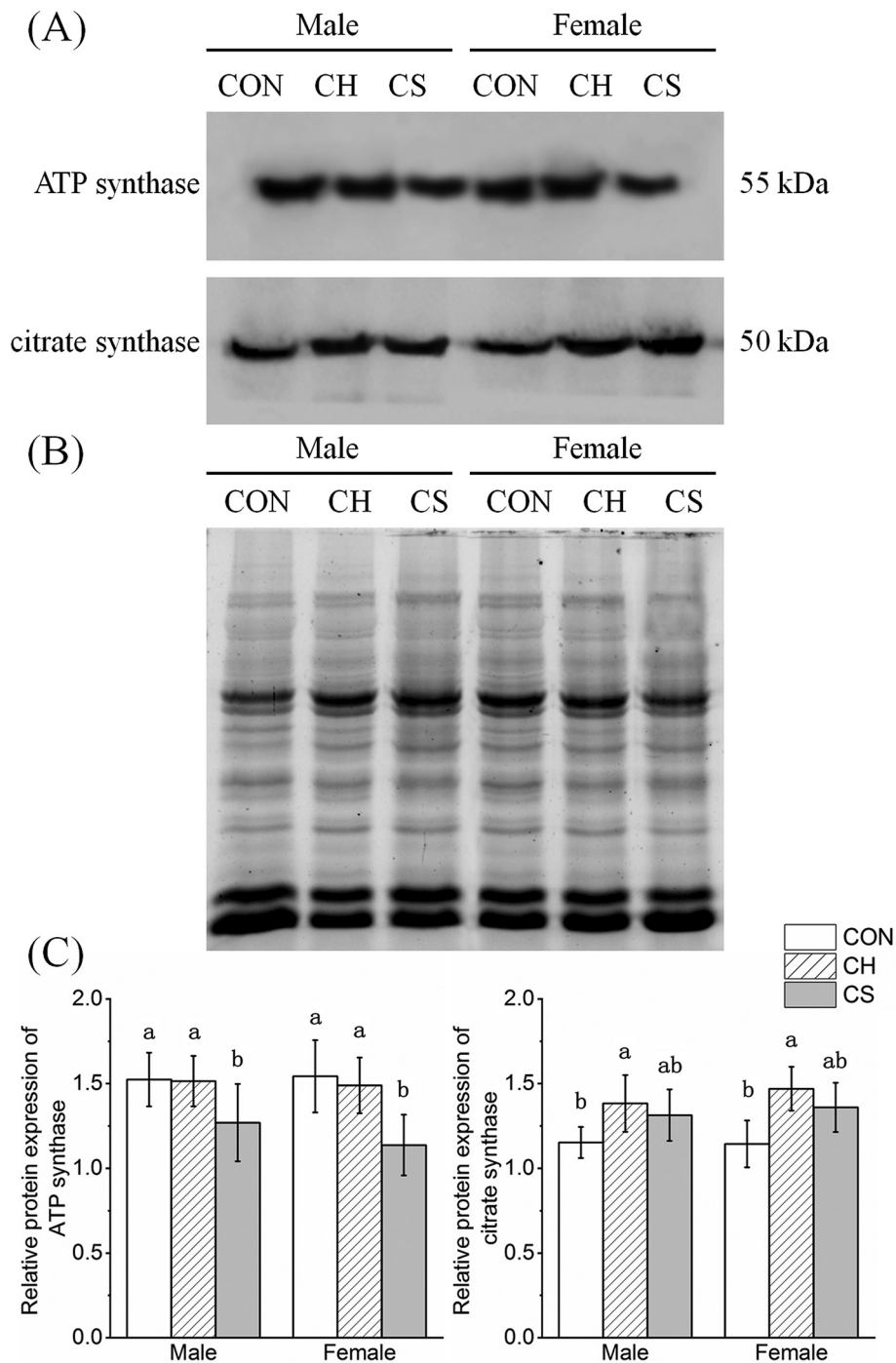


Fig. 6. Changes in protein expression levels of mitochondrial function-related factors in cardiac muscle of voles.

(A) Representative immunoblots of ATP synthase and citrate synthase in cardiac muscle. (B) Representative polyacrylamide gel of total protein. (C) Relative protein expression of ATP synthase and citrate synthase. Values are means \pm SD. $n = 8$. CON, control group; CH, cool huddling group; CS, cool separated group. Different letters indicate significant differences among temperature treatment groups ($P < .05$).

The relative protein expression level of ATP synthase in the CON and CH groups was significantly higher than that in the CS group. The relative protein expression of citrate synthases was higher in the CH group than that in the CON group ($P < .05$). There was no significant difference in the relative expression levels of the two proteins between males and females (Fig. 6C).

3.7. Changes in protein expression of apoptosis-related proteins

The relative protein expression of bax and bcl2 were detected by

Western blot analysis, as shown in Fig. 7A. Representative polyacrylamide gels of total protein are shown in Fig. 7B.

The ratio of bax to bcl2 was significantly higher in CH and CS groups than that in CON group, and the ratio was higher in females than that in males ($P < .05$) (Fig. 7C).

3.8. Changes in protein expression of mitochondrial autophagy-related proteins

The relative protein expression levels of PINK1, Parkin, and P-

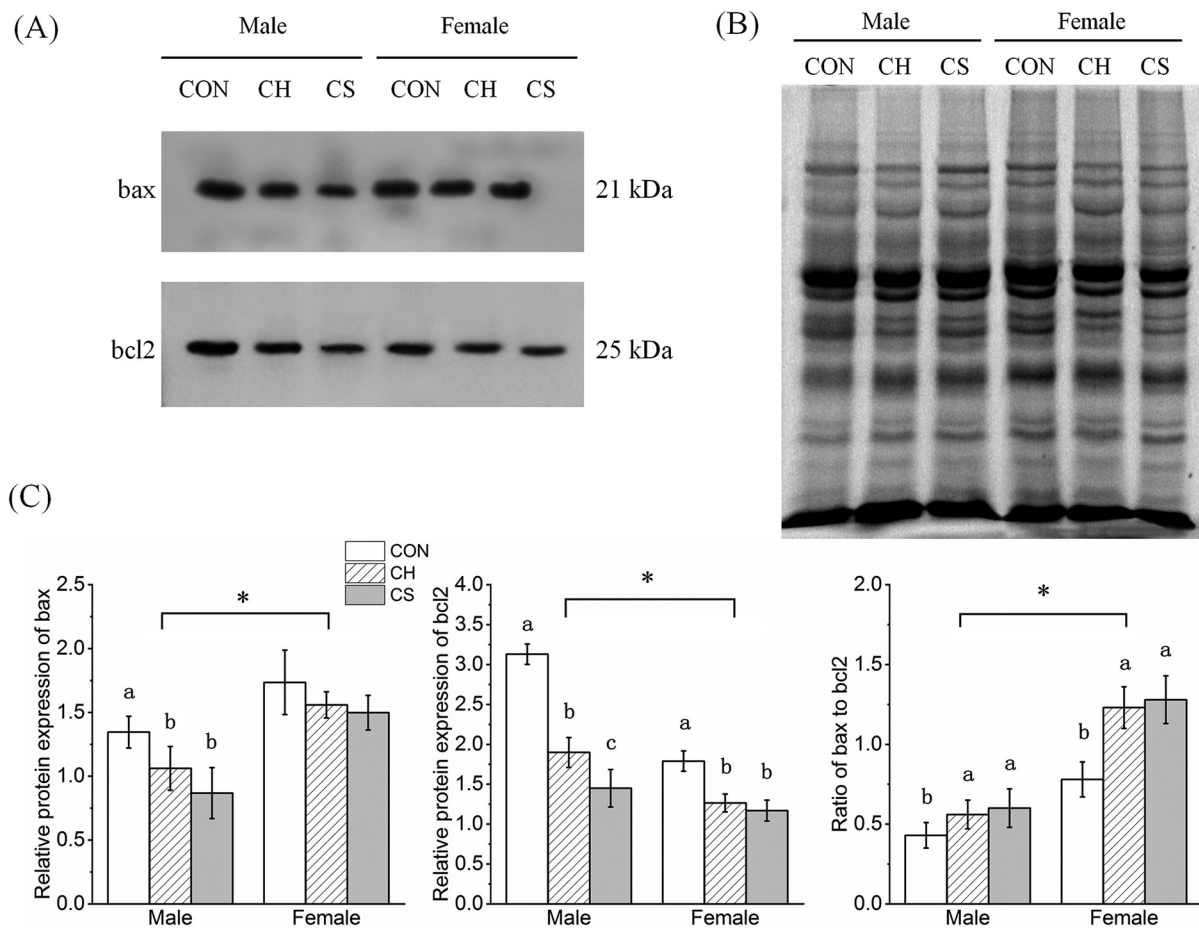


Fig. 7. Changes in protein expression levels of apoptosis-related factors in cardiac muscle of voles. (A) Representative immunoblots of bax and bcl2 in cardiac muscle. (B) Representative polyacrylamide gel of total protein. (C) Relative protein expression of bax, bcl2 and bax/bcl2. Values are means \pm SD. n = 8. CON, control group; CH, cool huddling group; CS, cool separated group. Different letters indicate significant differences among temperature treatment groups ($P < .05$). *, $P < .05$ significant differences between males and females.

Parkin were detected by western blot analysis, as shown in Fig. 8A. Representative polyacrylamide gels of total protein are shown in Fig. 8B.

The relative protein expression level of PINK1 and phosphorylation level of Parkin were significantly higher in the CH and CS groups than that in the CON group, and both values were higher in males than in females ($P < .05$) (Fig. 8C).

3.9. Changes in protein expression of mitochondrial fission-related proteins

The relative protein expression levels of DRP1, MFF, and FIS1 were detected by western blot analysis, as shown in Fig. 9A. Representative polyacrylamide gels of total protein are shown in Fig. 9B.

The relative protein expression levels of DRP1 and MFF were the highest in the CH group, whereas the relative protein expression level of FIS1 showed no significant differences among the three groups. There was no significant difference in the relative expression levels of DRP1 and MFF between males and females, whereas FIS1 expression was higher in males than that in females ($P < .05$) (Fig. 9C).

4. Discussion

We studied the effects of a cool environment on the number and function of cardiac mitochondria in huddling Brandt's voles, as well as the mechanism related to the balance of apoptosis, mitochondrial autophagy, and fission in regulating the number of mitochondria. Obvious mitochondrial damage was observed in the cardiac muscle of the CH

and CS groups, and the number of normal mitochondria in the two groups was less than 10% compared to that in the CON group. However, both the total number of mitochondria and the protein expression of ATP synthase in the CH group were higher than observed in the CS group. The protein expression of mitochondrial autophagy factor PINK1 and the phosphorylation of Parkin as well as apoptotic factor bax/bcl2 were significantly higher in the two cool groups (CH and CS) than that found in the CON group, and protein expression levels of mitochondrial fission factors DRP1 and MFF were significantly higher in the CH group than in the other two groups. DNA fragmentation and nuclear number showed no significant differences among the three treatment groups.

One of the most important findings in this study is that the number of normal myocardial mitochondria in voles under cool temperature decreased significantly, but the number of normal myocardial mitochondria in the CS group was even lower than that in the CH group. The total number of mitochondria (including normal and damaged mitochondria) in the CH group was the same as that in the CON group; whereas, the total number of mitochondria in the CS group was significantly decreased compared to that in the CON group. These results indicate that a lower degree of mitochondrial damage in the CH group than in the CS group under a cool environment. Previous studies have shown that the body temperature of huddling voles is slightly lower (about 1 °C) than that of separated voles when the environment is cool (Sukhchuluun et al., 2018), and a cold environment will lead to myocardial mitochondrial damage (Lushnikov and Nepomniashchikh, 1991); however, in this study, the myocardial mitochondria of the CH

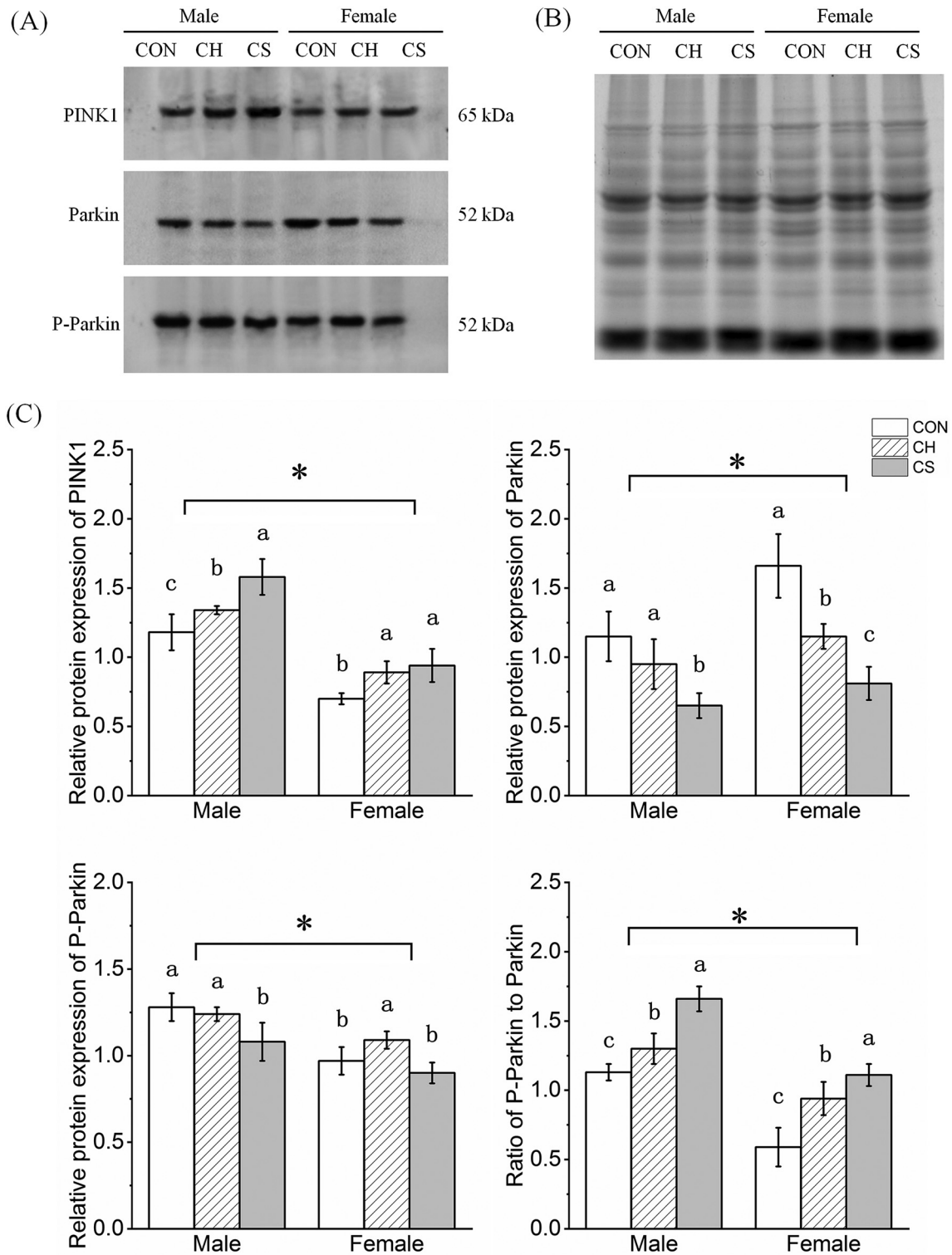


Fig. 8. Changes in protein expression levels of mitochondrial autophagy-related factors in cardiac muscle of voles. (A) Representative immunoblots of PINK1, Parkin, and P-Parkin in cardiac muscle. (B) Representative polyacrylamide gel of total protein. (C) Relative protein expression of PINK1, Parkin, P-Parkin, and P-Parkin/Parkin. Values are means ± SD. n = 8. CON, control group; CH, cool huddling group; CS, cool separated group. Different letters indicate significant differences among temperature treatment groups ($P < .05$). *, $P < .05$ significant differences between males and females.

group show better preservation, indicating that huddling is important for protecting the morphology and number of myocardial mitochondria in voles. In addition, the total number of myocardial mitochondria in voles of the two cool environment groups was slightly higher in males than in females. According to Bergmann's rule, the larger the animal's body size, the smaller the relative heat dissipation area, which is

conductive to resisting cold (Pincheira-Donoso, 2010; Vinarskii, 2013). We speculate that the gender differences in this study may be related to this rule, i.e., the larger the weight, the smaller the impact of a cool environment. In addition, the mean CSA of mitochondria did not change significantly among the three groups, but the standard deviation seemed to increase in the two cool groups, which may be related to the

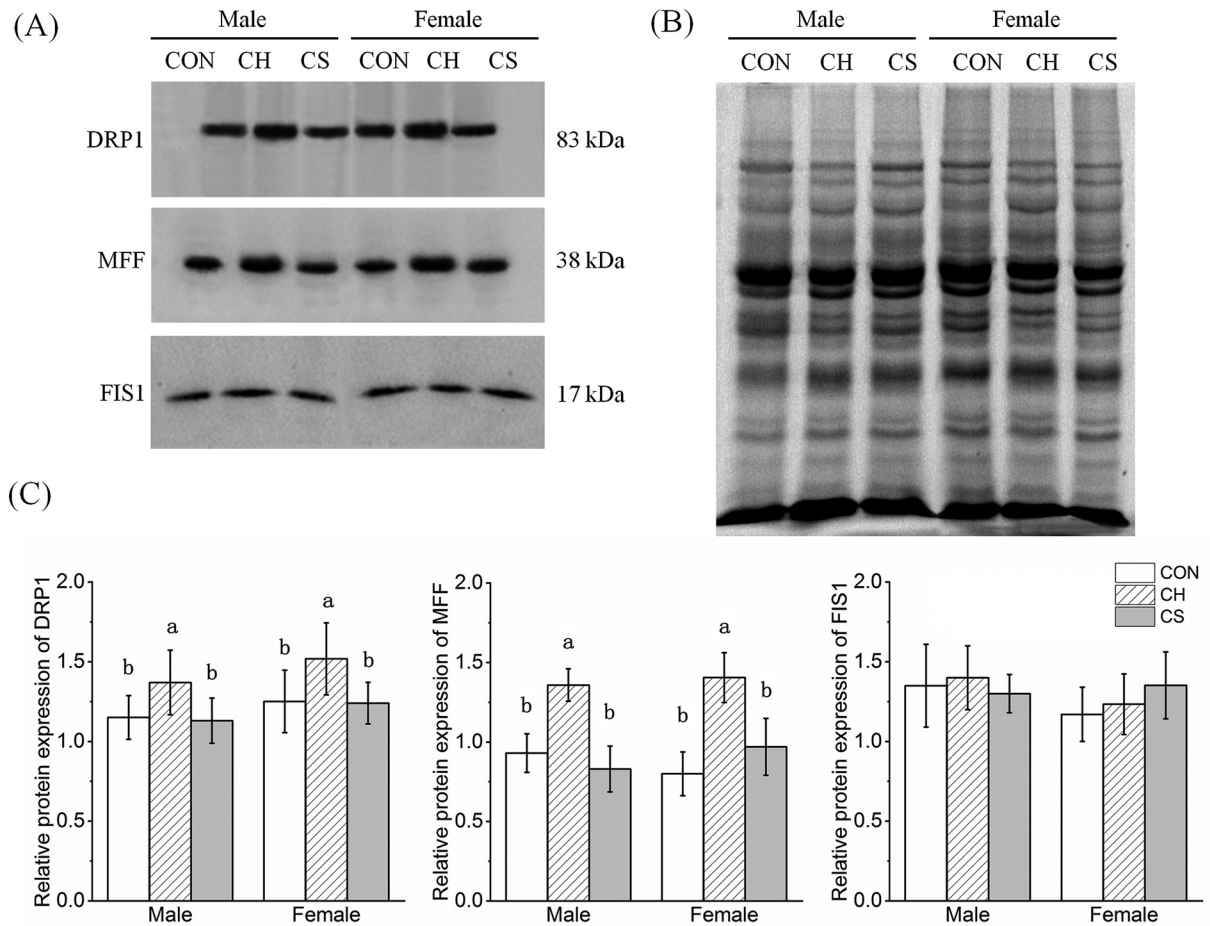


Fig. 9. Changes in protein expression levels of mitochondrial fission-related factors in cardiac muscle of voles.

(A) Representative immunoblots of DRP1, MFF, and FIS1 in cardiac muscle. (B) Representative polyacrylamide gel of total protein. (C) Relative protein expression of DRP1, MFF, and FIS1. Values are means \pm SD. $n = 8$. CON, control group; CH, cool huddling group; CS, cool separated group. Different letters indicate significant differences among temperature treatment groups ($P < .05$).

occurrence of both swelling and smaller mitochondria in the two cold groups.

Mitochondria mainly function in oxygen oxidation and energy supply, ATP synthase and citrate synthase are the key factors of them (Kramarova et al., 2008; Remington, 1992; Wiegand and Remington, 1986). In this study, ATP synthase protein expression and activity levels in the myocardium of CS voles were significantly reduced, whereas that of citrate synthase was unchanged, indicating that the ability of mitochondria to produce ATP may be weakened compared with that in the CON group. ATP synthase mainly synthesizes ATP, whereas uncoupling protein (UCP) is mainly responsible for heat production. Both use the proton of mitochondria to cross the membrane and antagonize each other in function (Busiello et al., 2015; Crichton et al., 2017). In this study, the low protein expression and activity level of ATP synthases in the CS group suggests that the ability of myocardial mitochondria to produce ATP may be weakened and may lead to increased thermogenesis. Although there is no report of ATP synthases in mammalian myocardium under cold environments, study on the myocardium of male Sprague-Dawley rats shows that the mRNA expression of UCP3 increases by 2–3 times under 5 °C, indicating an increase in myocardial heat production (Lin et al., 1998). The results of our experiment are similar, suggesting that myocardial mitochondrial function in the CS group exhibited significant adaptive changes under a cool environment due to the high plasticity of mitochondrial function. Interestingly, both citrate synthase and ATP synthase activity in the myocardium of voles in the cool huddling group remained unchanged compared with that in the CON group, indicating that aerobic oxidation and energy supply

capacity of mitochondria may remain stable. Thus, huddling may protect mitochondrial aerobic oxidation and ATP production in the myocardium of voles under cool environmental exposure. In view of previous studies, activity of Brandt's vole in the huddling group was significantly higher than that in the separated group under a cold environment (Sukhchuluun et al., 2018). We speculate that the protection of myocardial mitochondrial aerobic metabolism and ATP supply may be a basis for this phenomenon. In general, there was a significant adaptive change in myocardial mitochondrial function in the CS group, which may be partially offset by huddling.

To explore the mechanism of mitochondrial damage and alleviation, we first analyzed the mitochondrial autophagy factors. Results showed that the protein expression of PINK1 and the phosphorylation ratio of Parkin in the myocardium of the two cool groups were significantly higher than that of the CON group, indicating that the level of mitochondrial autophagy increased significantly and may be one of the main reasons for the decrease in the number of mitochondria. DRP1 is a key factor in mitochondrial fission, MFF up-regulates DRP1 activity, and overexpression of FIS1 inhibits mitochondrial fission (Mozdy et al., 2000; Tieu and Nunnari, 2000; Tilokani et al., 2018). In this study, the protein expression levels of DRP1 and MFF increased significantly in the cardiac muscle of the CH group, and FIS1 remained unchanged, suggesting that the mitochondrial fission level increased significantly at this time. We speculate that the increased levels of mitochondrial autophagy and fission in the CH group may promote the renewal of mitochondria, which may, in turn, help to alleviate the decrease in mitochondrial number and may be one of the reasons for the production of

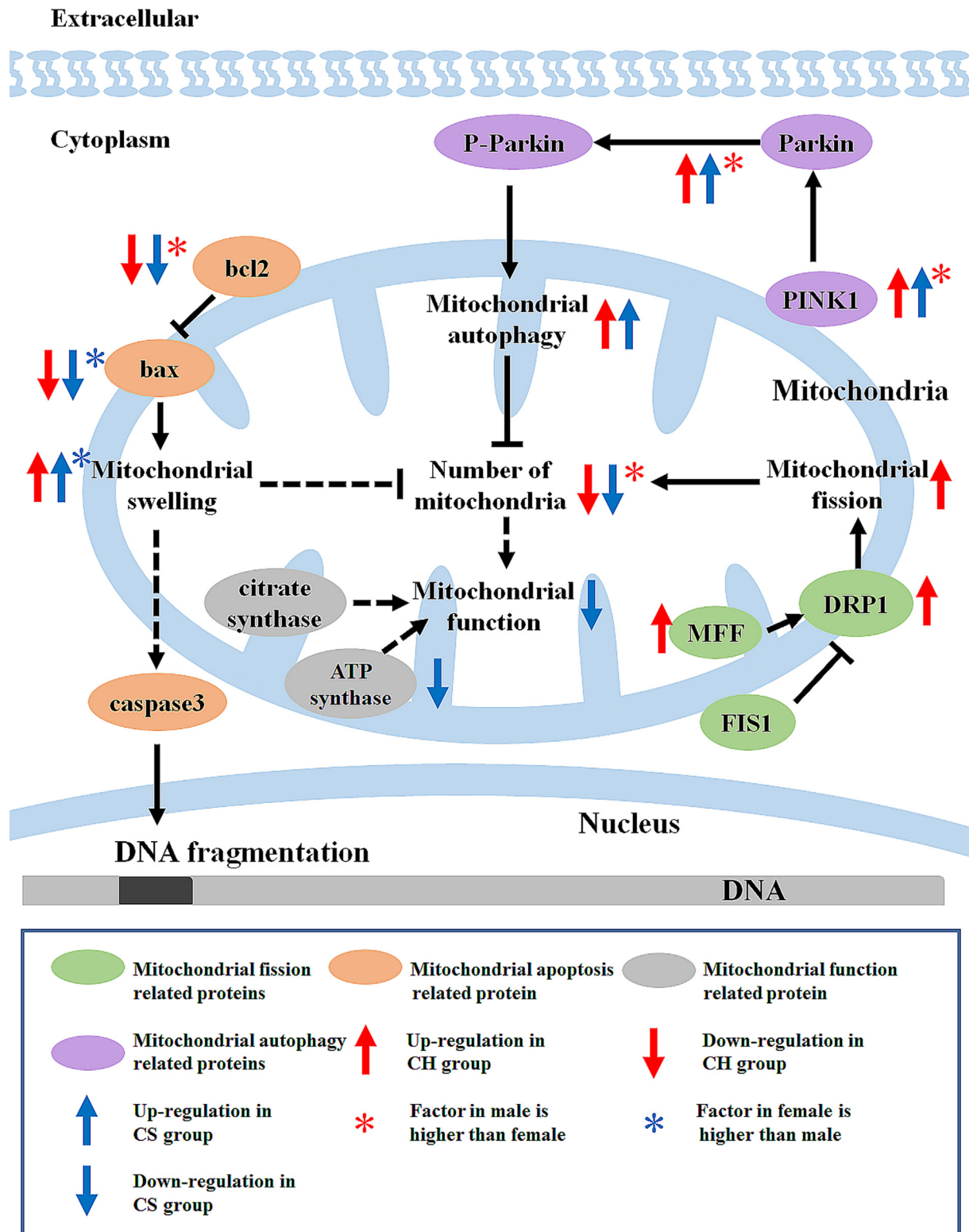


Fig. 10. Graphical summary of study.

ATP synthase, adenosine triphosphate synthase; DRP1, dynamin-related protein 1; MFF, mitochondrial fission factor; FIS1, fission 1; PINK1, PTEN induced putative kinase 1; Parkin, Parkinson's disease protein 2; CH, cool huddling group; CS, cool separated group.

new small mitochondria.

It should be noted that although the protein expression of bax/bcl2 increased in the two cool groups, no significant differences were observed among the three treatment groups in DNA fragmentation, nuclear number, or nuclear morphology. Bax can promote changes in

mitochondrial membrane permeability, leading to mitochondrial swelling and crista disorders (Antonsson et al., 1997; Korsmeyer et al., 1993). In this study, the increase in bax/bcl2 protein expression in the two cool groups may be one of the reasons for the structural damage observed in mitochondria, such as swelling and crista disorder, as well

as the impact on mitochondrial number to some extent. However, no significant differences were found in caspase3 activity among the three treatment groups. As caspase3 is the effector of apoptosis (Manickam et al., 2017), the stability of its activity may block bax-initiated apoptosis signals, which may help explain the stability of nuclear morphology and number in the myocardium of voles under cool conditions, and may be of great significance for the survival of animals in cool environments.

In summary, we explored the regulatory mechanism related to the balance of apoptosis, mitochondrial autophagy, and fission in regard to the structure, number, and function of myocardial mitochondria in huddling and separated Brandt's voles under a cool environment (Fig. 10). Results showed that a cool environment led to damage of myocardial mitochondria and reduction of mitochondrial number in voles, which could be partially alleviated by huddling behavior. Bax-induced mitochondrial structural damage and increased autophagy were identified as common mechanisms related to the reduction in myocardial mitochondria in voles under a cool environment, and the increase in mitochondrial fission may be one of the mechanisms used to alleviate the decrease in mitochondrial number. Furthermore, stability of caspase3 activity may play a role in the stability of apoptosis. Moreover, mitochondrial energy supply were higher in huddling voles than in separated voles, which may be an adaptive change caused by the collective overwintering behavior of socialized animals. The main difference between the sexes was a higher number of myocardial mitochondria in males than in females, which may be due to the high protein expression level of bax/bcl2 in female voles. In general, the increased mitochondrial fission level in huddling voles partly counteracted the decrease in myocardial mitochondria caused by the increase in autophagy, and maintenance of caspase3 activity protected the nucleus from mitochondrial damage induced by bax.

Funding

This work was supported by funds from the National Natural Science Foundation of China (No. 31770455, 31670385, 31570377).

Data availability statement

The datasets and original images are included in the supplementary document.

Disclosures

No conflicts of interest, financial or otherwise, are declared by the authors.

Author contributions

Z.W., J.-H.X., and L.-X.X. conceived and designed the research; Z.W., J.-H.X., J.-J.M., X.-T.K., and J.-W.Z. performed the experiments; Z.W. analyzed the data; Z.W. interpreted the experimental results; Z.W. and J.-J.M. prepared the figures; Z.W. and J.-H.X. drafted the manuscript; M.W. and H.-L.X. provided experimental guidance and suggestions for revision; Z.W. and J.-H.X. edited the manuscript and approved the final version of the manuscript.

References

Antonsson, B., Conti, F., Ciavatta, A., Montessuit, S., Lewis, S., Martinou, I., Bernasconi, L., Bernard, A., Mermoud, J.J., Mazzei, G., Maundrell, K., Gambale, F., Sadoul, R., Martinou, J.C., 1997. Inhibition of Bax channel-forming activity by Bcl-2. *Science* 277, 370–372.

Biazik, J., Vihinen, H., Anwar, T., Jokitalo, E., Eskelinen, E.L., 2015. The versatile electron microscope: an ultrastructural overview of autophagy. *Methods (San Diego, Calif.)* 75, 44–53.

Busiello, R.A., Savarese, S., Lombardi, A., 2015. Mitochondrial uncoupling proteins and

energy metabolism. *Front. Physiol.* 6, 36.

Chavez, L.O., Leon, M., Einav, S., Varon, J., 2017. Editor's choice- inside the cold heart: a review of therapeutic hypothermia cardioprotection. *Eur. Heart J. Acute Cardiovasc. Care* 6, 130–141.

Crichton, P.G., Lee, Y., Kunji, E.R., 2017. The molecular features of uncoupling protein 1 support a conventional mitochondrial carrier-like mechanism. *Biochimie* 134, 35–50.

Douglas, T.K., Cooper, C.E., Withers, P.C., 2017. Avian torpor or alternative thermoregulatory strategies for overwintering? *J. Exp. Biol.* 220, 1341–1349.

Dugbartey, G.J., Hardenberg, M.C., Kok, W.F., Boerema, A.S., Carey, H.V., Staples, J.F., Henning, R.H., Bouma, H.R., 2017. Renal mitochondrial response to low temperature in non-hibernating and hibernating species. *Antioxid. Redox Signal.* 27, 599–617.

Fang, H., Chen, M., Ding, Y., Shang, W., Xu, J., Zhang, X., Zhang, W., Li, K., Xiao, Y., Gao, F., Shang, S., Li, J.C., Tian, X.L., Wang, S.Q., Zhou, J., Weisleder, N., Ma, J., Ouyang, K., Chen, J., Wang, X., Zheng, M., Wang, W., Zhang, X., Cheng, H., 2011. Imaging superoxide flash and metabolism-coupled mitochondrial permeability transition in living animals. *Cell Res.* 21, 1295–1304.

Fekkes, P., Shepard, K.A., Yaffe, M.P., 2000. Gag3p, an outer membrane protein required for fission of mitochondrial tubules. *J. Cell Biol.* 151, 333–340.

Fu, W.W., Hu, H.X., Dang, K., Chang, H., Du, B., Wu, X., Gao, Y.F., 2016. Remarkable preservation of Ca²⁺ homeostasis and inhibition of apoptosis contribute to anti-muscle atrophy effect in hibernating Daurian ground squirrels. *Sci. Rep. U.K.* 6, 13.

Gilbert, C., McCafferty, D., Le Maho, Y., Martrette, J.M., Giroud, S., Blanc, S., Ancel, A., 2010. One for all and all for one: the energetic benefits of huddling in endotherms. *Biol. Rev. Camb. Philos. Soc.* 85, 545–569.

Jefimow, M., Glabska, M., Wojciechowski, M.S., 2011. Social thermoregulation and torpor in the Siberian hamster. *J. Exp. Biol.* 214, 1100–1108.

Kane, L.A., Lazarou, M., Fogel, A.I., Li, Y., Yamano, K., Sarraf, S.A., Banerjee, S., Youle, R.J., 2014. PINK1 phosphorylates ubiquitin to activate Parkin E3 ubiquitin ligase activity. *J. Cell Biol.* 205, 143–153.

Kelly, F.E., Nolan, J.P., 2010. The effects of mild induced hypothermia on the myocardium: a systematic review. *Anaesthesia* 65, 505–515.

Kenny, H.C., Rudwill, F., Breen, L., Salanova, M., Blottner, D., Heise, T., Heer, M., Blanc, S., O'Gorman, D.J., 2017. Bed rest and resistive vibration exercise unveil novel links between skeletal muscle mitochondrial function and insulin resistance. *Diabetologia* 60, 1491–1501.

Korsmeyer, S.J., Shutter, J.R., Veis, D.J., Merry, D.E., Oltvai, Z.N., 1993. Bcl-2/Bax: a rheostat that regulates an anti-oxidant pathway and cell death. *Semin. Cancer Biol.* 4, 327–332.

Kotze, J., Bennett, N.C., Scantlebury, M., 2008. The energetics of huddling in two species of mole-rat (Rodentia: Bathyergidae). *Physiol. Behav.* 93, 215–221.

Kramarova, T.V., Shabalina, I.G., Andersson, U., Westerberg, R., Carlberg, I., Houstek, J., Nedergaard, J., Cannon, B., 2008. Mitochondrial ATP synthase levels in brown adipose tissue are governed by the c-Fo subunit P1 isoform. *FASEB J.* 22, 55–63.

Kraus, F., Ryan, M.T., 2017. The constriction and scission machineries involved in mitochondrial fission. *J. Cell Sci.* 130, 2953–2960.

Li, R., Shen, Y., 2013. An old method facing a new challenge: re-visiting housekeeping proteins as internal reference control for neuroscience research. *Life Sci.* 92, 747–751.

Lin, B., Coughlin, S., Pilch, P.F., 1998. Bidirectional regulation of uncoupling protein-3 and GLUT-4 mRNA in skeletal muscle by cold. *Am. J. Physiol. Endocrinol. Metab.* 275, E386–E391.

Liu, R., Chan, D.C., 2015. The mitochondrial fission receptor Mff selectively recruits oligomerized Drp1. *Mol. Biol. Cell* 26, 4466–4477.

Lushnikov, E.L., Nepomniashchikh, L.M., 1991. An ultrastructural stereological analysis of the myocardium in homoiothermal animals during cooling. *Biull. Eksp. Biol. Med.* 111, 214–217.

Manickam, P., Kaushik, A., Karunakaran, C., Bhansali, S., 2017. Recent advances in cytochrome c biosensing technologies. *Biosens. Bioelectron.* 87, 654–668.

Michalska, B., Duszynski, J., Szymanski, J., 2016. Mechanism of mitochondrial fission-structure and function of Drp1 protein. *Postepy Biochem.* 62, 127–137.

Mozdy, A.D., McCaffery, J.M., Shaw, J.M., 2000. Dnm1p GTPase-mediated mitochondrial fission is a multi-step process requiring the novel integral membrane component Fis1p. *J. Cell Biol.* 151, 367–380.

Namekata, S., Geiser, F., 2009. Effects of nest use, huddling, and torpor on thermal energetics of eastern pygmy-possums. *Aust. Mammal.* 31, 31–34.

Nowack, J., Geiser, F., 2016. Friends with benefits: the role of huddling in mixed groups of torpid and normothermic animals. *J. Exp. Biol.* 219, 590–596.

Nunez-Villegas, M., Bozinovic, F., Sabat, P., 2014. Interplay between group size, huddling behavior and basal metabolism: an experimental approach in the social degu. *J. Exp. Biol.* 217, 997–1002.

Otera, H., Ishihara, N., Mihara, K., 2013. New insights into the function and regulation of mitochondrial fission. *BBA Mol. Cell Res.* 1833, 1256–1268.

OuYang, Q., Tao, N., Zhang, M., 2018. A damaged oxidative phosphorylation mechanism is involved in the antifungal activity of Citral against *Penicillium digitatum*. *Front. Microbiol.* 9, 239.

Pincheira-Donoso, D., 2010. The balance between predictions and evidence and the search for universal macroecological patterns: taking Bergmann's rule back to its endothermic origin. *Theory Biosci.* 129, 247–253.

Polderman, K.H., 2009. Mechanisms of action, physiological effects, and complications of hypothermia. *Crit. Care Med.* 37, S186–S202.

Posch, A., Kohn, J., Oh, K., Hammond, M., Liu, N., 2013. V3 stain-free workflow for a practical, convenient, and reliable total protein loading control in western blotting. *J. Visual. Exp.* 50948.

Remington, S.J., 1992. Structure and mechanism of citrate synthase. *Curr. Top. Cell. Regul.* 33, 209–229.

Reynolds, E.S., 1963. The use of lead citrate at high pH as an electron-opaque stain in

- electron microscopy. *J. Cell Biol.* 17, 208.
- Scantlebury, M., Bennett, N.C., Speakman, J.R., Pillay, N., Schradin, C., 2006. Huddling in groups leads to daily energy savings in free-living African four-striped grass mice, *Rhabdomys pumilio*. *Funct. Ecol.* 20, 166–173.
- Song, M., Chen, F.F., Li, Y.H., Zhang, L., Wang, F., Qin, R.R., Wang, Z.H., Zhong, M., Tang, M.X., Zhang, W., Han, L., 2018. Trimetazidine restores the positive adaptation to exercise training by mitigating statin-induced skeletal muscle injury. *J. Cachexia. Sarcopenia Muscle* 9, 106–118.
- Sukhchuluun, G., Zhang, X.Y., Chi, Q.S., Wang, D.H., 2018. Huddling conserves energy, decreases Core body temperature, but increases activity in Brandt's voles (*Lasiopodomys brandtii*). *Front. Physiol.* 9, 563.
- Tessier, S.N., Storey, K.B., 2012. Myocyte enhancer factor-2 and cardiac muscle gene expression during hibernation in thirteen-lined ground squirrels. *Gene* 501, 8–16.
- Tieu, Q., Nunnari, J., 2000. Mdv1p is a WD repeat protein that interacts with the dynamin-related GTPase, Dnm1p, to trigger mitochondrial division. *J. Cell Biol.* 151, 353–366.
- Tilokani, L., Nagashima, S., Paupe, V., Prudent, J., 2018. Mitochondrial dynamics: overview of molecular mechanisms. *Essays Biochem.* 62, 341–360.
- Treat, M.D., Scholer, L., Barrett, B., Khachatryan, A., McKenna, A.J., Reyes, T., Rezazadeh, A., Ronkon, C.F., Samora, D., Santamaria, J.F., Rubio, C.S., Sutherland, E., Richardson, J., Lighton, J.R.B., van Breukelen, F., 2018. Extreme physiological plasticity in a hibernating basoendothermic mammal, *Tenrec ecaudatus*. *J. Exp. Biol.* 221, 9.
- Vinarskiĭ, M.V., 2013. On the application of Bergmann's rule to ectothermic organisms: the state of the art. *Zhurnal Obs. Biol.* 74, 327–339.
- Wang, Z., Jiang, S.F., Cao, J., Liu, K., Xu, S.H., Arfat, Y., Guo, Q.L., Chang, H., Goswami, N., Hinghofer-Szalkay, H., Gao, Y.F., 2019. Novel findings on ultrastructural protection of skeletal muscle fibers during hibernation of Daurian ground squirrels: mitochondria, nuclei, cytoskeleton, glycogen. *J. Cell. Physiol.* 234, 13318–13331.
- Wang, Z., Xu, J.H., Mou, J.J., Kong, X.T., Wu, M., Xue, H.L., Xu, L.X., 2020. Photoperiod affects Harderian gland morphology and secretion in female *Cricetulus barabensis*: autophagy, apoptosis, and mitochondria. *Front. Physiol.* 11, 408.
- Wiegand, G., Remington, S.J., 1986. Citrate synthase: structure, control, and mechanism. *Annu. Rev. Biophys. Biophys. Chem.* 15, 97–117.
- Wojciechowski, M.S., Jefimow, M., Pinshow, B., 2011. Heterothermy, and the energetic consequences of huddling in small migrating passerine birds. *Integr. Comp. Biol.* 51, 409–418.
- Xu, D.-L., Xu, M.-M., Wang, D.-H., 2019. Effect of temperature on antioxidant defense and innate immunity in Brandt's voles. *Zool. Res.* 40, 305–316.
- Xu, Y., Yao, Y., Jiang, X., Zhong, X., Wang, Z., Li, C., Kang, P., Leng, K., Ji, D., Li, Z., Huang, L., Qin, W., Cui, Y., 2018. SP1-induced upregulation of lncRNA SPRY4-IT1 exerts oncogenic properties by scaffolding EZH2/LSD1/DNMT1 and sponging miR-101-3p in cholangiocarcinoma. *J. Exp. Clin. Cancer Res.* 37, 81.
- Yamano, K., Matsuda, N., Tanaka, K., 2016. The ubiquitin signal and autophagy: an orchestrated dance leading to mitochondrial degradation. *EMBO Rep.* 17, 300–316.
- Zhang, X.Y., Sukhchuluun, G., Bo, T.B., Chi, Q.S., Yang, J.J., Chen, B., Zhang, L., Wang, D.H., 2018. Huddling remodels gut microbiota to reduce energy requirements in a small mammal species during cold exposure. *Microbiome* 6, 103.